Canopy Reflectance Model Inversion in Multiple Forward Mode: Forest Structural Information Retrieval from Solution Set Distributions

S.A. Soenen, D.R. Peddle, C.A. Coburn, R.J. Hall, and F.G. Hall

Abstract

Remote estimation of canopy structure is important in forestry and a variety of environmental applications. Multiple Forward Mode (MFM) look-up table (LUT) inversion of canopy reflectance models is one approach for obtaining forest canopy biophysical-structural information (BSI). MFM provides inversion results from models that are not invertible directly, and has advantages in terms of software requirements, model complexity, computational demands, and provision of physically-based BSI output. Proper handling of MFM-LUT parameterization and inherent uncertainty in the inversion procedure at the critical final BSI retrieval stage is essential, and is the theme of this paper. Three approaches are presented for deriving BSI from MFM-LUT multiple solution sets: reflectance equality (REQ), nearest spectral distance (NSD), and spectral range domain (SRD). These approaches were validated at a Rocky Mountain test site, for which SRD corresponded best with field data, with RMSE 0.4 m and 0.8 m obtained for horizontal and vertical crown radius, respectively. Recommendations for selecting MFM inversion approaches are provided for future applications.

Introduction

Remote estimation of forest canopy structure is important in forest inventory and plays a key role in forest fire modeling, forest management, carbon estimates, and climate change studies (Hall, 1999; Franklin, 2001; UNFCCC, 2004; Patenaude *et al.*, 2005). Forest stand characteristics obtained by remote sensing image analysis and modeling (e.g., canopy dimensions, stand density, fraction of cast shadow) can be related to a number of important biophysical variables including canopy volume and bulk density (Riano *et al.*, 2004), stem volume (Pilger *et al.*, 2003), biomass (Fournier *et al.*, 2003), and leaf area (Peddle *et al.*, 2004). These biophysical parameters are important in afforestation, reforestation, and deforestation contexts in countries committed to sustainable development and international carbon reporting (Brown, 2002) as well as more generally for monitoring and change detection applications (Gong and Xu, 2003). Further, remote sensing is recognized as an important approach to derive biophysical-structural information (BSI) required as Essential Climate Variables (ECV; see UNFCCC, 2004) in international global climate change agreements (e.g., the Kyoto Protocol; UNFCCC, 1997) because of opportunities to obtain systematic, repetitive information at local to global scales with archival imagery dating back to baseline years (e.g., Kyoto in 1990) that is critical in carbon accounting and policy compliance (Rosenqvist *et al.*, 2003; Patenaude *et al.*, 2005).

Canopy reflectance models link airborne and satellite image spectral response with the biophysical and structural composition of a forest canopy. These models are comprehensive in describing explicitly and quantitatively the main parts of the system being measured by a remote sensing instrument, that is, the bidirectional reflectance of forest canopies as a function of canopy structure, illumination and viewing positions, surface geometry, landscape component spectral properties, and sub-pixel scale abundance (Strahler, 1997).

Compared to other methods, most canopy reflectance models have an explicit physical basis and thus, a fundamental advantage over traditional empirical methods that are mired in a purely statistical domain. For example, empirical relationships between canopy structural parameters and vegetation indices are influenced by factors including: inconsistency over varying cover types, mixed pixel problems, limited spectral dimensionality (typically only two bands), non-comprehensive biophysical characterization (e.g., saturation at higher LAI), an inability to account for variability in the following: canopy cover, illumination and canopy geometry, leaf optical properties

S.A. Soenen, D R. Peddle, and C.A. Coburn are with the Department of Geography, University of Lethbridge, 4401 University Drive West, Lethbridge, AB, T1K 3M4, Canada (derek.peddle@uleth.ca).

R.J. Hall is with the Canadian Forest Service, Northern Forest Centre, 5320 - 122 Street, Edmonton, AB, T6H 3S5, Canada, and the Department of Geography, University of Lethbridge, AB, Canada.

F.G. Hall is with NASA Goddard Space Flight Center, Code 614.4, 8800 Greenbelt Rd., Greenbelt MD 20771.

Photogrammetric Engineering & Remote Sensing
Vol. 75, No. 4, April 2009, pp. 361–374.

0099-1112/09/7504–0361/$3.00/0

at sub-pixel scales, as well as being poorly suited for variable canopy densities (Sellers, 1985; Curran and Williamson, 1987; Guyot *et al.*, 1989; Spanner *et al.*, 1990; Lathrop and Pierce, 1991; Bannari *et al.*, 1995; Hall *et al.*, 1995 and 1996; McDonald *et al.*, 1998; Peddle *et al.*, 1999 and 2001a).

These problems are overcome using canopy reflectance models based on the comprehensive, physically-based system modeling approach (Strahler *et al.*, 1997). There are two main types of reflectance model use: forward mode (structural inputs: output is modeled reflectance) and inverse mode (pixel reflectance is input: the model produces BSI outputs). Conceptually, model inversion is clearly preferred, since it yields the required BSI of interest, as reviewed by Chen *et al.* (2000) for a variety of models. In this paper, we extend model inversion based on previously established multiple forward mode (MFM) procedures (Peddle *et al.*, 2003a and 2004) as a hybrid forward-inverse approach that overcomes major limitations of direct or iterative model inversion, as explained below, and we test and present preferred methods to handle multiple-solution sets generated from this approach.

Direct inversion of physically-based canopy reflectance models is a complex task due to the larger number of variables and processes, and sensitivity to error inherent in remote measurements of surface radiance (Kimes *et al.*, 2000). Many approaches exist to achieve mathematical model inversion with a wide array of applications, as described in Strahler (1997), Chen *et al.* (2000), and Kimes *et al.* (2000). In remote sensing forestry applications, the development of more sophisticated mathematical models of forest canopy reflectance presents a powerful context for obtaining BSI results. A challenge, and in some cases a limitation to viable inversion in this context, however, is that the increased complexity and number of variables considered creates the potential for indeterminate systems of equations, thus rendering inversion intractable or impossible. This presents the dilemma that the increased sophistication required to more properly model the system has the unfortunate result of rendering that model non-invertible due to its complexity (i.e., it can be run in forward-mode only). Further, inversion procedures are computationally intense for large data sets containing multiple images covering large areas, or multi-temporal and multi-angular data sets. The amount of computational resources required for these types of studies also increases with model complexity. Thus, traditional inversion methods are currently not fully compatible with the scope of environmental information needs and the requirements of remote sensing and canopy reflectance model inversion over large areas due to the inordinate computational requirements and intractable mathematical demands. To satisfy these information needs, it is likely that hybrid inversion approaches (Schlerf and Atzberger, 2006), genetic algorithms (Fang *et al.*, 2003), or the simple and efficient look-up table method (Kimes *et al.*, 2000) are required.

Look-up table (LUT) inversion methods for canopy reflectance models provide a practical solution to the problems found in traditional inversion techniques (Kimes *et al.*, 2000; Weiss *et al.*, 2000; Combal *et al.*, 2002; Peddle *et al.*, 2003a). Within these methods, modeled canopy reflectance is pre-computed from forward mode model runs for a range of potential BSI conditions that are stored together with the input structural parameters in a set of LUTs. Indirect LUT inversion is then the process of matching measured reflectance values from remote sensor imagery with modeled reflectance as stored in the LUT. Consequently, the model is not directly inverted mathematically and instead needs to be run in forward mode only. Advantages of this includes (a) additional inversion algorithms are not required (i.e., optimization), (b) any level of model complexity can be used, including highly sophisticated models that are not directly invertible, (c) less computational constraints, with data storage and input-output requirements still manageable, and, (d) provision of practical processing strategies to provide flexibility and additional power to the user through options for physically-based forest analysis by remote sensing.

The objective of this paper, therefore, is to present new and more refined methods for handling the parameterization and LUT inversion stage for final BSI retrieval, test and validate these methods in a rigorous forest experiment, and provide criteria and recommendations for selecting which strategy to use. This builds on and compares previous developments (Kimes *et al.*, 2000; Weiss *et al.*, 2000; Peddle *et al.*, 2003a, 2003b, and 2004) in which indirect methods of model inversion were implemented and represented a significant advance in BSI retrieval with remote sensing. In addition, this paper focuses on the description of multiple solutions which has, until recently, been ignored or only addressed in a limited way, and is thus a significant gap and need in realizing comprehensive LUT-based indirect inversion. In this paper, the issues of input structural parameter selection, search constraints, and most importantly, the description and selection of canopy structure estimates from a set of potential inversion solutions are addressed. Methods for achieving this are first presented, and then tested using SPOT imagery with field validation for a mountain forest study area in the Canadian Rocky Mountains.

Multiple Forward Mode Reflectance Modeling and Inversion

Look-up table (LUT) methods involving canopy reflectance modeling have been implemented, studied and used successfully by a variety of investigators (Knyazikhin *et al.*, 1998; Weiss *et al.*, 2000; Combal *et al.*, 2002; Gastellu-Etchegorry *et al.*, 2003; Peddle *et al.*, 2004 and 2007). The Multiple-Forward-Mode (MFM) method of inverting canopy reflectance models with LUTs used in this study was developed by Peddle *et al.* (2003a, 2003b, 2003c, 2004, and 2007) and has been validated at a variety of ecosystems for obtaining different types of forest BSI using different models and sensors. MFM is a suite of tools for LUT inversion of canopy reflectance model output that automates both LUT parameterization and search. With MFM, the user provides input parameters and ranges for a series of standard forward mode canopy reflectance model executions. If these are not known *a priori*, they can be generated automatically, permitting any area to be analyzed without field or other knowledge (Peddle *et al.*, 2007). The MFM algorithm then varies the structural input values systematically according to these user-specified or automatically-generated parameter ranges (e.g., minimum and maximum crown radius, stand density, LAI, and tree height) and increment steps. The results of sequential runs of the canopy reflectance model are stored in a LUT. The inversion to retrieve BSI information first involves searching the LUT for modeled reflectance values that match with airborne or satellite image reflectance data, and secondly, retrieving the corresponding structural input data from the LUT (e.g., crown dimension, density, and LAI) that generated the actual modeled reflectance value that matches with the image pixel value.

Parameterization: The Inversion Space

Kimes *et al.* (2000) describe the LUT inversion concept in terms of three attributes:

1 An instrument specific space *D* consisting of individual observations of canopy reflectance (*d*);

2. A canopy realization space P consisting of all possible realizations of canopy structure (χ), leaf optical properties (ω), and background or understory reflectance (ρ), such that an individual element, $p = (\chi, \omega, \rho)$; and
3. A relationship F between the two spaces where $D = F(P) = \{F(P): p \in P\}$.

Accordingly, the inversion problem for an individual observation (d) is to find all p for which $F(p) = d$. In simple terms, $F(p)$ is the modeled reflectance using p as input, which is matched with observed reflectance d. To achieve solutions for all $d \in D$ it is necessary to characterize P with a suitable level of detail. However, determining an appropriate amount of detail is not straight forward, is often ignored, and can be application or data set specific. Other LUT inversion methods have relied on a set of functions for each input parameter to characterize the area of $F(P)$ occupied by the forest canopy. These functions are derived according to model sensitivity to each input parameter so that the spectral domain is systematically sampled. These functions are necessarily model-specific given that different models have different input parameters, and, for simplicity, it is assumed that input parameter effects on model output are independent or that there is no co-variance, consistent with other work (Weiss *et al.*, 2000). Aside from accommodating different input parameters unique to a given model, the MFM approach is otherwise not specific to any model and indeed has been used with a variety of canopy reflectance models, as demonstrated in previous work (e.g., Peddle *et al.*, 2003a, 2004, and 2007). In terms of input specification, if general inventory data are available, this can used as reference, otherwise, the MFM approach can be run without any *a priori* information using a multi-step process whereby a general set of input parameters is refined based on initial inversion results (Peddle *et al.*, 2007). Pre-screening of the LUTs and simple ecosystem specific physical constraint rules may optionally be applied to limit or remove untenable structural parameter input combinations prior to the application of the search algorithm for inversion. Alternatively, when used in situations where no *a priori* knowledge is available for a given area, MFM provides, in essence, an unsupervised capability. This is a common requirement for large regional, continental or global scale studies where field work is prohibitive, diversity is high, and other input sources do not exist, are unavailable, or are impractical to use. As long as the MFM-LUT is suitably populated (which, for large-areas in "blind" tests is achieved by simply specifying a large range on the first iteration), the method can be used in any location or setting. In a second (final) iteration, the ranges are reduced according to initial search results, and parameter increments are then increased to provide proper detail (precision) for final retrieval. An important issue, however, is quantifying optimal increments (precision) for acceptable BSI retrieval, while not creating LUTs of excessive size that may impact search algorithm efficiency, introduce redundancy, and result in slower MFM run-times. A key component of this paper is thus assessing the trade-off between complexity (detail) within the LUT as a result of large or small increment and range sizes and BSI retrieval accuracy, a subject that has received limited attention in the literature.

Inversion: Matching Modeled and Measured Reflectance

MFM inversion has typically been executed on the assumption that an exact match between model and measured reflectance values can be found, assuming limited model and calibration uncertainty (Peddle *et al.*, 2003b). This LUT search method is described here as reflectance equality (REQ). The use of reflectance equality as match criteria for indirect inversion has been used extensively in past inversion studies (Chen *et al.* 2000, Kimes *et al.* 2000, Peddle *et al.*, 2003a, 2003b, 2003c, and 2004). Within the REQ method, the measured and modeled reflectances are scaled to whole number values. Any structural parameter set (p) that produces a modeled reflectance that matches the measured reflectance becomes a potential BSI inversion result. In the REQ method there may be a single match, no direct match, or multiple matches. A case with no direct matches may result from an insufficient level of complexity in P. As mentioned earlier, this may be a matter of computational limits. Conversely, multiple matches may, in part, result from over-sampling of model spectral space in LUT creation.

A second method of search uses a measure of spectral distance defined with the relative Root Mean Square Error ($RMSE_{rel}$) to determine the closest matching modeled reflectance values, referred to here as nearest spectral distance (NSD) (Weiss *et al.*, 2000):

$$RMSE_{rel} = \sqrt{\frac{1}{n_b}\sum_{i=1}^{n_b}\left(\frac{\rho_i - \hat{\rho}_i}{\rho_i}\right)^2} \quad (1)$$

where n_b is the number of spectral bands, ρ is measured reflectance, and $\hat{\rho}$ is modeled reflectance for a constant solar and viewing position at the time of image acquisition. A minimum of two spectral bands are necessary for indirect inversion, however, this number may be increased to include all, or any combination of spectral bands measured by a sensor. This equation is used over a classical RMSE equation when the user prefers not to place emphasis on bands that have the largest absolute reflectance values (Weiss *et al.*, 2000). The use of the NSD equation is analogous to the merit function in optimization techniques. Under ideal imaging and modeling conditions, choosing a single potential inversion solution based on the NSD should be effective for predicting canopy structural parameters. If the canopy reflectance was accurately modeled and there was little or no error in calibrated image data, then the extracted model input structural parameters should closely correspond to conditions observed *in situ*. To obtain an exact match, modeled reflectance values must correspond to the precision dictated by the radiometric resolution of a given sensor. Within the MFM framework, the radiometric distribution and precision of output modeled reflectance values is dictated by the ranges and increment steps of the structural and other inputs, and thus there is potential for regions in the spectral domain where modeled and measured values do not coincide. Therefore, NSD may be used exclusively in place of REQ to account for any discrepancy between modeled and measured reflectance due to issues of instrument and MFM modeling precision.

An alternative method is to select all records where the spectral distance is within a set spectral range domain (SRD) as defined by Equation 1, similar to the method described by Weiss *et al.* (2000). In this method, a preliminary test is applied with a small subset of image pixels with known structure where records are extracted and ranked based on Equation 1 and BSI retrieval error. The lowest average BSI retrieval error is compared with the number of records extracted with the RMSE value used as the limiting criteria. The RMSE value corresponding to the lowest BSI retrieval error is then used as the limit criteria for the remainder of LUT searches. This MFM matching approach is well suited for coupled studies involving a variety of ecosystems, multiple sensors and different reflectance models, since it avoids sensor and model specific attempts to characterize error, system noise, and complex, potentially non-linear and spatially varying landscape factors. In this approach, it is essential that multiple solution sets be handled properly, and with options to enable appropriate multiple solution set processing, as described in the next section.

Multiple Solution Set Processing

In the case of multiple solutions, a number of procedures may be used to characterize or reduce these matches. In some applications, such as BSI inputs to carbon/water/energy models, it may be acceptable to specify a range of structural values as the MFM output. For broader spatial scale applications, this may be more representative of reality both in terms of model precision and spatial variability on the ground. In most other situations, however, it is desirable to provide one solution (be it a value or assignment to a class) or a summary statistic for a given pixel inversion. Central tendency has been used extensively in past studies to summarize inversion results and reduce dimensionality when multiple solutions occur (Weiss *et al.*, 2000; Combal *et al.*, 2002; Peddle *et al.*, 2003a, 2003b, and 2004). In the implementation of MFM described here, two methods exist to reduce these potential solutions. This first uses statistical measures such as central tendency and variance to describe the distribution of reflectance values in the solution set; and thus reduces the effects of instrument measurement and MFM model precision. The second method incorporates ancillary information (e.g., elevation, slope, aspect from a digital elevation model (DEM)) to further limit the potential solutions to those that match both reflectance and ancillary conditions. It is important to note that while the value being extracted using central tendency is taken as the "solution" and used for validation purposes, the actual "true value" may be found anywhere within the distribution of potential solutions and that (a) the dispersion of this distribution can be taken as a measure of estimate uncertainty (Kimes *et al.*, 2000), and (b) the accuracy reported from validation may under-estimate the true information content resident in the LUT and the BSI retrieval potential.

Inversion within Domains of Uncertainty

There is a level of uncertainty inherent in both $F(p)$ and D as current remote measurements are prone to instrument measurement variance and canopy reflectance models also vary in their ability to simulate canopy reflectance. Kimes *et al.* (2000) define two domains of uncertainty around measured and modeled reflectance where the "true value" may be found: the domain of uncertainty O_F for $F(p)$, and the domain O_d for d. As a result, a number of potential solutions to the inversion problem may be found since there is a number of p in O_F that are comparable to values found within O_d. The structural elements that yield these potential matches can then be described in terms of structural parameter distribution functions, or, if a single structural value is desired, any of the previously described procedures to handle multiple solutions may be used.

As described earlier, using the SRD retrieval method, it is possible to conduct a preliminary test to determine the appropriate retrieval domain (i.e., $RMSE_{rel}$) within Equation 1. The domains can be approximated by an n_b-dimensional boundary with axis δ marking the extent of uncertainty in each band for a given set of illumination and view angles. Thus, the domains would be equivalent to: $\rho \pm \delta_{\text{measured}}$ and $\hat{\rho} \pm \delta_{\text{model}}$. It is most effective to use known or published error values to calculate the extent of the domain; however, it is also possible to calculate potential measurement uncertainty (Kimes *et al.*, 2000). In this paper, we relate the domain of uncertainty to the range condition imposed in Equation 1.

MFM Inversion Validation: Experimental Design

Study Area

The MFM solution set inversion approaches were tested in an area of complex mountainous terrain in the Canadian Rocky Mountains. The study area was centered at 51.02° N, 115.07° W and included a montane/sub-alpine forest ecoregion along the eastern slopes of the front range of the Rocky Mountains in Kananaskis Country Provincial Park, Alberta, Canada (Figure 1). The elevation ranges from 1,400 m to 2,100 m with a full range of terrain aspects, and slopes ranging from 0° to 55°. The study area included montane and sub-alpine vegetation zones (Archibald *et al.*, 1996). The forested parts of the study area that formed the focus of this analysis were dominated by stands of lodgepole pine (*Pinus contorta* var. *latifolia* Dougl ex. Loud.).

Dataset

Values for d were taken from a cloud free, orthorectified SPOT5 (Systeme pour l'Observation de la Terre) satellite image of the Kananaskis study area acquired on 12 August 2004 with a spatial resolution of 10 m. Positional error was found to be less than one-half pixel. The SPOT data were converted to reflectance using published gain values and a correction for atmospheric effects using the empirical line method (Smith and Milton, 1999). A comparison of calibrated image reflectance and measured reflectance of a pseudo-invariant image feature (a parking lot; see Milton *et al.*, 1997) that covered the spatial equivalent of four image pixels showed the difference in reflectance measured was within 2 percent for all SPOT bands, similar to results reported by Milton *et al.* (1997) and Smith and Milton (1999). The SPOT data were resampled to 25 m to match the resolution of an associated digital elevation model (DEM). Elevation, slope, and aspect data were derived from the DEM.

Structural data were collected from 25 field plots (400 m^2). The plot size was selected to contain image pixels used in the MFM inversion, with plot coordinates obtained in the field using differentially-corrected GPS. The primary structural parameters of interest in this example application were horizontal and vertical crown radius, following previous studies in this area that focused on MFM applications in topographic correction (Soenen *et al.*, 2005), land-cover (Soenen *et al.*, 2007), and canopy density, forest

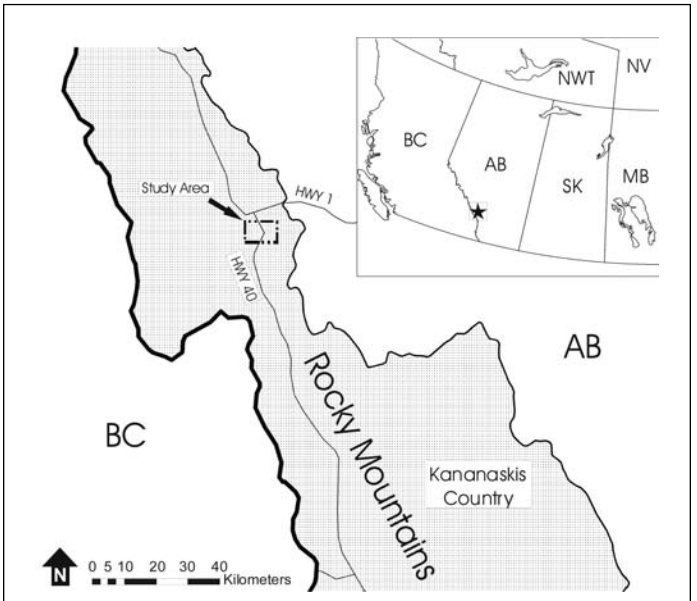

Figure 1. Montane/Sub-Alpine study area in Kananaskis Country, Alberta on the front range of the Canadian Rocky Mountains.

TABLE 1. DESCRIPTIVE STATISTICS FOR MEASURED HORIZONTAL CROWN RADIUS (r), VERTICAL CROWN RADIUS (b) FOR 25 CONIFER FIELD PLOTS

	r (m)	b (m)
Mean	1.0	3.0
S.D.	0.4	1.2
Minimum	0.2	0.5
Maximum	3.1	8.4

height, and volume retrieval (Pilger *et al.*, 2003). Horizontal crown radius was measured in the field using a two step process. First, a densiometer was used to determine the vertical projection of the horizontal extent of the crown to the ground. Then, a tape measure was used to measure the horizontal extent from the projected canopy center. This was repeated for another axis measurement at a right angle to the first to ascertain within-crown horizontal crown radius variability. The two measurements were averaged to provide the final field estimate of horizontal crown radius (Table 1). Vertical crown radius was determined using a digital hypsometer or a clinometer and simple geometric calculations (Table 1). The data were collected for all trees within each 400 m^2 plot area and used to validate the BSI retrieval results from the MFM inversion procedure.

Canopy Reflectance Model

In this study, the physically-based Li and Strahler (1992) geometric-optical mutual shadowing (GOMS) canopy reflectance model was used within the MFM framework. The GOMS model was chosen due to its computational efficiency, its accuracy for different forest types and scales (Schaff *et al.*, 1994, Li and Strahler, 1992, Abuelgasim and Strahler, 1994, Schaff and Strahler, 1994), its inclusion of slope and aspect which is an important consideration in mountainous areas (Gemmel, 1998), and based on results from an earlier comparison of GOMS with other models (Peddle *et al.*, 1999).

The GOMS model treats individual canopy elements (tree crowns) as discrete spheroids with a Poisson model random spatial distribution for a given density (λ) on a spectrally contrasting background. The orientation and size of the spheroids are defined by inputs of horizontal (r) and vertical crown radius (b), height to the center of the crown (h) and the distribution of height within the pixel area (dh). The model uses parallel-ray geometric calculations to determine the sub-pixel scale fractions of sunlit background (B), sunlit canopy (C) with Lambertian reflective properties, and shadow (S) cast on neighboring crowns and background. The pixel-scale reflectance is modeled based on the end-member spectra for the reflectance components (ρ_b, ρ_c, ρ_s) weighted by their projected area fractions within the pixel for a given set of illumination and view geometries. The effect of terrain orientation is also taken into account in GOMS (Schaff *et al.*, 1994), and thus, slope and aspect model inputs were available in MFM. Based on earlier work by Abuelgasim and Strahler (1994) and Schaff and Strahler (1994) using the GOMS model (Li and Strahler, 1992), model uncertainty was assessed to be within 1 percent reflectance for visible bands, and within 4 percent for NIR and SWIR bands for this type of forested region.

TABLE 2. MFM-GOMS MODEL INPUTS FOR ILLUMINATION AND VIEW ANGLE FOR KANANASKIS COUNTRY, ROCKY MOUNTAINS, ALBERTA, CANADA FOR SPOT SATELLITE IMAGE ACQUISITION DATE (12 AUGUST 2004)

Illumination and View Angle	
Solar Zenith Angle	37°
Solar Azimuth Angle	157°
View Zenith Angle	7°
View Azimuth Angle	15°

MFM Runs: Parameterization Sets

In this study, the space P was populated using two MFM protocols for a constant set of view and illumination angles (Table 2) to isolate and compare the effect of varied canopy structure inputs. In the first set (MFM Run 1 and 2; Table 3), a general range of input parameters was used based on limits of possible canopy realizations. In the second, *a priori* structural information taken from field data in the Kananaskis study area was used to constrain P. In this second protocol (MFM Run 3 and 4; Table 4), two standard deviations from the mean of each model input parameter was used to set the range of inputs. It was also possible to remove untenable structural conditions. For example, in the field data no cases exist where $r > b$, thus all cases where r > b were removed from the LUT. Any redundant LUT entries were also removed. The increment for parameter ranges in both protocols was varied between coarse and fine steps yielding four LUT sets. Spectral endmember data (ω, ρ) were collected in the field using a high spectral resolution spectroradiometer for sunlit lodgepole pine canopy, sunlit understory background, and shadow (Table 5) and related to SPOT image spectral response using published spectral response functions. The reflectance data were calibrated using spectralon (PTFE) panel measurements and calibration coefficients following protocols developed by Peddle *et al.* (2001b). Endmember spectra showed little within-species-type variation and thus each endmember reflectance value was held constant during LUT creation. This contributed to maintaining a reasonable LUT size and consequently, computation time.

It was possible to visually examine the effect of these different parameter distributions on the resulting modeled reflectance in the space co-occupied by D. Figure 2 shows a simple two band example from validation plot pixels in the SPOT image (Figure 2a) and modeled reflectance from the four MFM runs (Table 3 and Table 4). A direct relationship exists between the complexity of P and the modeled reflectance coverage within the inversion space. Consequently, it was likely there would be no exact solution for many $d \in D$ where input parameter complexity was low (i.e., MFM Runs 1 to 3) and reflectance equality was used as the match criteria. In many forestry applications, however, it is not necessary to acquire exact structural information at the precision required to have each d equate to a complex $F(p)$ (Peddle *et al.*, 2003b). Instead, it is common to associate d with a class or range of parameters or to have p within some error tolerance (i.e., SRD).

Inversion Tests

The MFM inversion procedure was tested using a variable input structure. Four MFM-LUTs, containing $F(p)$ and p were used alternately within the inversion procedure. Reflectance input values (d) were taken from SPOT bands 2 and 3 for one analysis set and from all SPOT bands for the second analysis set. In these analysis sets, slope and aspect values derived from the DEM were used to constrain potential matches in a third analysis set to cases where $F(p) = d$, and cases where the DEM-derived slope and aspect matched slope and aspect found in p. Structural values selected for evaluation were horizontal and vertical crown radius (r and b, respectively), since these had the most detailed and accurate field data and thus represented the most rigorous validation. Structural values were selected from the LUT using one of three selection criteria: (a) NSD, (b) REQ, and (c) SRD. The

TABLE 3. STRUCTURAL PARAMETER RANGES AND INCREMENTS FOR THE GOMS MODEL: MFM RUN 1 AND MFM RUN 2

Structural Parameter	MFM run 1			MFM run 2		
	Min	*Max*	*inc*	*Min*	*Max*	*inc*
Density - λ (trees/m^2)	0.05	0.55	0.1	0.05	0.5	0.05
Horizontal Crown Radius - r (m)	0.5	6.5	2	0.5	6.5	1
Vertical Crown Radius - b (m)	0.5	6.5	2	0.5	6.5	2
Height to Crown Center - h (m)	5	15	5	4	14	2
Height Distribution - dh (m)	5	25	10	5	25	5
Slope - α (°)	0	60	20	0	60	10
Aspect - φ (°)	0	315	45	0	315	45
LUT Size (Combinations)		31104			529200	

TABLE 4. STRUCTURAL PARAMETER RANGES AND INCREMENTS FOR THE GOMS MODEL: MFM RUN 3 AND MFM RUN 4

Structural Parameter	MFM run 3			MFM run 4		
	Min	*Max*	*inc*	*Min*	*Max*	*inc*
Density - λ (trees/m^2)	0.05	0.25	0.05	0.06	0.26	0.02
Horizontal Crown Radius - r (m)	0.5	2.5	1	0.5	2.5	0.5
Vertical Crown Radius - b (m)	1	4	1	1	4	1
Height to Crown Center - h (m)	10	14	1	10	14	1
Height Distribution - dh (m)	5	15	5	6	16	2
Slope - α (°)	0	40	10	0	40	5
Aspect - φ (°)	0	315	45	0	315	45
LUT Size (Combinations)		40500			445500	

TABLE 5. SPECTRAL INPUTS FOR THE GOMS MODEL

Endmembers	ρ_{SWIR}	ρ_{NIR}	ρ_{RED}	ρ_{GREEN}
Sunlit Pine Canopy	0.168	0.487	0.041	0.061
Sunlit Spruce Canopy	0.083	0.411	0.055	0.071
Sunlit Background (Pine, Spruce)	0.333	0.243	0.086	0.061
Shadow	0.013	0.072	0.005	0.012

spectral domain limit was compared using initial inversion tests to find the lowest potential estimate error based on Weiss *et al.* (2000). The results from each of the selection criteria were compared. Any solution set retrieved using REQ and SRD was described using two measures of central tendency (mode and median) together with a full description of the solution distribution (i.e., full distribution of values for each BSI parameter).

Validation and Comparison

The goal of the comparison of prediction error was to examine the effect of LUT complexity, input data structure, solution selection criteria, and description of multiple solutions when selecting a single structural result using central tendency (mode, median). The estimate accuracy for BSI values (i.e., *r* and *b*) was assessed using absolute root mean square error (RMSE) between estimated and actual values for the 25 conifer validation plots:

$$RMSE = \sqrt{\frac{1}{n}\sum_{i=1}^{n}(x - x_m)^2} \quad (2)$$

where x is the model predicted structural value, x_m is the measured structural value, and n is the number of validation plots. The second section of this study also examines the distribution of multiple solutions for a sample set of validation plots.

Results and Discussion

Results are divided into three sections based on the limiting method used for selection of potential matches (i.e., NSD, REQ, and SRD). Within these sections, the benefits of using other constraint methods (multiple bands, DEM) are discussed along with the measures of central tendency used to select an inversion result from the distribution (median, mode). The efficacy of the inversion methods presented above was evaluated based on agreement between field-measured canopy element dimensions and values extracted from solution distributions from the LUT inversion procedure.

Estimates of Structure Using the REQ Retrieval Method

The best estimates of *r* and *b* were obtained using SPOT band 2 and 3 and the parameterization with larger increment sizes and input parameter ranges refined using a priori information (Table 6). The estimate error was 0.8 m for *r* and 0.9 m for *b* using this parameterization. Parameterizations with ranges not refined using *a priori* information (i.e., MFM run 1, MFM run 2) resulted in higher estimate error and the use of the median description of multiple solutions was generally less than the mode. The use of a finer increment step size did not improve estimates, but also did not increase estimate error in *r* and *b* more than 0.2 m and 0.4 m, respectively. These results indicate that in REQ, estimate error increases with parameterizations that have a higher potential for multiple solutions. Neither measure of central tendency sufficiently reduces the estimate error for these parameterizations. Thus, a large number of the multiple solutions likely contain BSI information that does not reflect conditions in the validation plots, indicating that very different BSI information

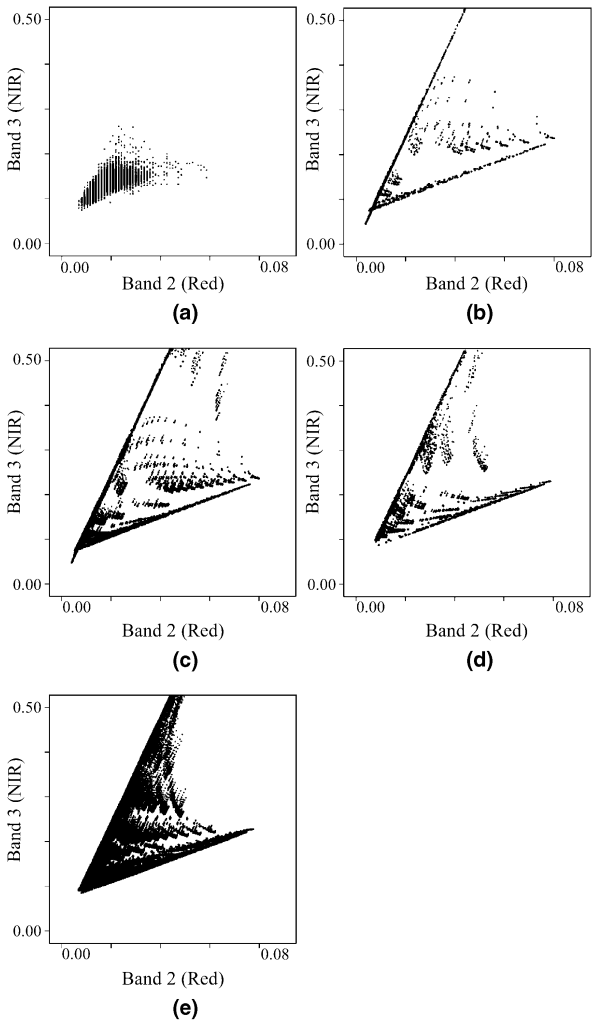

Figure 2. Two band plots of (a) a sample of observed reflectance and modeled reflectance using varied inputs from: (b) MFM Run1, (c) Run 2, (d) Run 3, and (e) Run 4.

combinations will yield reflectance values that are similar according to the REQ method.

The use of slope and aspect to constrain solutions did not decrease estimate error within the REQ retrieval in all cases and resulted in a larger number of validation plots with no solution. The inclusion of additional spectral bands reduced the overall prediction error; however, it also increased the number of validation plots with no solution. This suggested that the level of modeled reflectance coverage within the spectral space co-occupied by the measured reflectance was too low in some areas where values of measured canopy reflectance were still present (Figure 2).

Estimates of Structure Using the NSD Retrieval Method

The best overall BSI estimates using NSD criteria were obtained with SPOT band 2 and 3, and parameterizations refined using a priori information (Table 7). The NSD estimates of *r* were more accurate than REQ for all parameterizations, while the estimates of *b* were similar or improved. The BSI estimates were within an error margin that closely corresponded to the increment size for the structural parameters evaluated. Error for horizontal canopy radius (*r*) estimates was between 1.2 m and 1.7 m for MFM run 1 (increment: 2 m), between 0.6 m and 1.1 m for MFM run 2 (increment 1 m), 0.6 m and 0.8 m for MFM run 3 (increment 1 m) and 0.4 m and 0.7 m for MFM run 4 (increment 0.5 m). For smaller increment sizes, the mean error values became closer to the increment size and it was likely that a threshold value existed where error would cease to decrease with increasing increment precision. This may suggest that the BSI estimate error using NSD was dependant on the sampling increment of *P*, in a way opposite to the REQ method. This observation also applied to the vertical crown radius estimates where estimate error was within 2 m for MFM run1 and MFM run 2, and close to 1 m for MFM run 3 and MFM run 4.

The number of input spectral bands also had an effect on the inversion results using the closest spectral distance method. A decrease in mean estimate error for *r* was observed for all MFM scenarios when all SPOT bands were used in the inversion procedure. The decrease in absolute RMSE was most substantial for the MFM-LUTs with larger input parameter increments and ranges. Again, this

TABLE 6. ABSOLUTE RMSE FROM ESTIMATED HORIZONTAL (*r*) AND VERTICAL (*b*) CROWN RADIUS USING REFLECTANCE VALUE MATCHES. BOLD VALUES INDICATE LOWEST ABSOLUTE RMSE WHERE ALL VALIDATION PLOTS INCLUDED INVERSION SOLUTIONS (I.E., CASES WITH NO MATCHES = 0)

		Absolute RMSE				
		r (m)		b (m)		
	Input Bands	median	mode	median	mode	no matches
MFM Run 1	2,3	3.0	1.6	1.4	1.3	3
	2,3, slope, aspect	3.2	2.8	1.5	1.4	3
	1,2,3,4	0.2	0.2	0.3	0.3	23
	1,2,3,4, slope, aspect	–	–	–	–	25
MFM Run 2	2,3	2.3	1.9	0.9	1.0	3
	2,3, slope, aspect	2.2	1.8	0.9	1.0	3
	1,2,3,4	2.9	2.7	0.9	0.9	14
	1,2,3,4, slope, aspect	0.1	0.1	0.2	0.2	24
MFM Run 3	2,3	**0.8**	**0.8**	**0.9**	**0.9**	0
	2,3, slope, aspect	0.9	0.9	0.7	0.8	2
	1,2,3,4	0.3	0.3	0.5	0.5	14
	1,2,3,4, slope, aspect	0.2	0.2	0.2	0.2	23
MFM Run 4	2,3	0.9	1.0	1.0	1.1	0
	2,3, slope, aspect	0.9	0.9	1.0	1.3	1
	1,2,3,4	0.3	0.3	0.9	0.9	12
	1,2,3,4, slope, aspect	0.3	0.2	0.8	0.8	18

TABLE 7. ABSOLUTE RMSE FROM ESTIMATED HORIZONTAL (*r*) AND VERTICAL (*b*) BROWN RADIUS USING CLOSEST SPECTRAL DISTANCE. BOLD VALUES INDICATE LOWEST ABSOLUTE RMSE

		Absolute RMSE	
	Input Bands	r (m)	b (m)
MFM Run 1	2,3	1.7	1.7
	2,3, slope, aspect	1.3	1.7
	1,2,3,4	1.3	1.6
	1,2,3,4, slope, aspect	1.2	1.2
MFM Run 2	2,3	0.9	1.3
	2,3, slope, aspect	1.1	1.6
	1,2,3,4	0.6	0.9
	1,2,3,4, slope, aspect	0.8	1.1
MFM Run 3	2,3	0.7	**0.8**
	2,3, slope, aspect	0.6	0.9
	1,2,3,4	0.6	1.0
	1,2,3,4, slope, aspect	0.8	1.0
MFM Run 4	2,3	0.5	1.1
	2,3, slope, aspect	0.6	1.1
	1,2,3,4	**0.4**	1.3
	1,2,3,4, slope, aspect	0.7	1.17

suggests that there is a maximum level of accuracy that may be achieved through using fine input parameter increments beyond which improvements by using additional techniques are minimal or negligible. For vertical crown radius, the use of additional input channels only improved the results for the first two LUT sets (MFM run 1, MFM run 2). The error levels remained similar in the LUT sets where *a priori* data were used to limit the inputs (MFM run 3, MFM run 4). The use of terrain input channels did not consistently improve the structural estimates beyond the minimum estimate error in *r* and *b*. Overall error for estimates derived using terrain input channels was within 0.4 m RMSE of estimates derived without terrain inputs.

Estimates of Structure Using the SRD Retrieval Method

In this study, the retrieval limit in Equation 1 was systematically varied to examine the effect of spectral domain size on estimate error. It was expected that, with decreasing domain size, the distribution of potential solutions would narrow and that the median or mode value would shift. As the distribution narrowed, the difference between the measured and estimated structure would decrease to a minimum point. At this point, it was assumed that the domain of uncertainty would closely approximate that found in the measured and modeled reflectance data set, which was considered desirable. This was confirmed by minimum absolute RMSE for structural values occurring at similar error domain sizes when comparing the two band and four band input results across the two LUT sets. The lowest estimate error for r occurred when the RMSE limit in Equation 1 was set between 0.05 and 0.1 for 2 bands and 0.35 and 0.4 for 4 bands. This is similar to the evaluated RMSE when measured and model uncertainty (δ) maxima are added to the terms within Equation 1 (Figure 2a and Figure 3a). The relationship between *b* estimate error and the RMSE limit was less defined (Figure 2b and Figure 3b).

Comparing the structural estimates using error domains to those using closest spectral distance showed the absolute structural estimate error reaching levels equivalent to closest spectral distance. For example, the minimum absolute structural RMSE for MFM run 4 horizontal crown radius estimates using SRD were all below 0.5 m while the NSD estimates were within 0.7 m (Figure 4). The results were similar for vertical crown radii with overall estimate error within 1 m for minimum values using the error domain method and within 1.3 m for the closest spectral distance method. In some cases, such as MFM run 2, the horizontal crown radius estimate error using four input bands was considerably higher for the spectral domain method, with the closest spectral distance method showing an RMSE improvement greater than 1 m. The estimate error was also lower when using the median value from the solution distribution in most cases.

It was likely that this error domain method was only effective when LUTs with a high sampling density within *P* were used. In LUTs with high information content it was possible to retain a larger distribution of values at smaller error domains that were less susceptible to influences of erroneous potential solutions and more characteristic of conditions on the ground. These distributions may also contain information about canopy structural variance. This is a topic for future research.

Structural Estimates: Assessment of Individual Plots

Additional perspective was gained from detailed examination of structural estimates for individual plots. The majority of estimates were within 0.5 m of the averaged crown dimensions measured on the ground. The difference between estimated and actual structural values revealed no general trend to the prediction error, with the exception of the REQ-based estimates of horizontal crown radius where the estimates were consistently higher than the measured values (Figure 5). For horizontal crown radius, the percentages of estimates falling within 0.5 m difference of the averaged measured value were as follows: 72 percent of the estimates for the NSD method, 36 percent with the REQ method, and 80 percent with the method using SRD. For vertical crown radius, the percentage of estimates falling within 0.5 m difference was: 56 percent for the NSD method, 72 percent for the REQ method, and 60 percent for the SRD method. The maximum error was 1.7 m for *r* and 3.6 m for *b*, both occurring within the REQ method (Figures 5 and 6).

There were consistently high levels of difference between measured and estimated structure regardless of estimate method for a few of the 25 test plots (e.g., validation plots 4, 7, and 8). Since a wide range of canopy conditions were found within the distributed validation plots, some conditions within these validation plots were outside the distribution bounds used to generate the restricted (2σ) LUT sets (e.g., MFM Run 3 and MFM Run 4). For example, structural estimates for validation plot 4 showed consistently high error regardless of estimation method. In that plot, while the horizontal and vertical crown radii were within the distribution of values present in the LUT, the stem density was outside the range of LUT inputs (3,025 stems/ha). The structural estimates from this inversion procedure were in error as the true structural conditions were not represented within the potential solutions. The inversion procedure still selected a set of potential solutions; however, the matching reflectance was generated by a set of structural conditions that were biased since the field structural parameter was not found within the range of values input to the model.

Solution Distributions

The previous sections have reported levels of error based on the assumption that a central tendency description of potential solutions is optimal. These measures of central tendency, however, are based on likelihood and may not fully describe the true effectiveness of the inversion method. If there is agreement between the field-measured structural value and a value within the distribution of potential

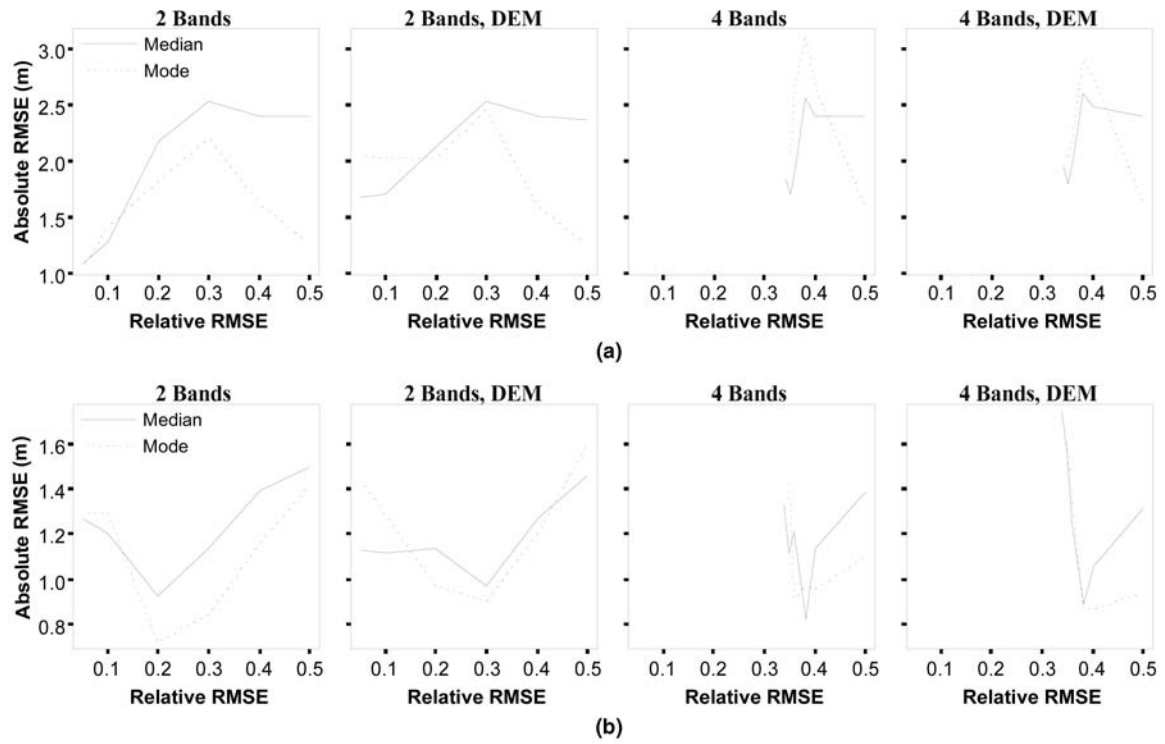

Figure 3. Absolute RMSE between structural estimates of horizontal crown radius (a), vertical crown radius (b) and field measured values for 25 conifer plots using values from MFM Run 2. Relative RMSE in the spectral domain between measured and modeled reflectance was increased systematically to simulate different domains of uncertainty. The results show the change in structural estimation error with large and refined domains of uncertainty.

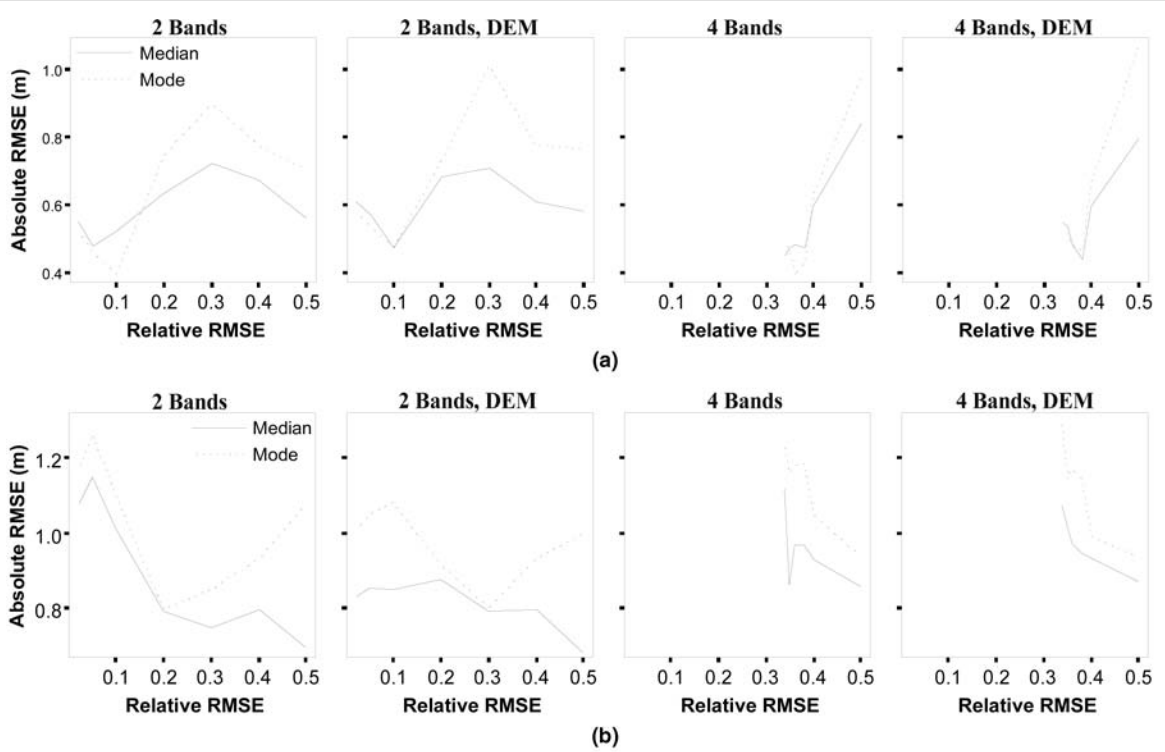

Figure 4. Absolute RMSE between estimates of horizontal crown radius (a), vertical crown radius (b) and field measured values for 25 conifer plots using values from MFM Run 4. Relative RMSE between measured and modeled reflectance was varied to simulate different domains of uncertainty. The results show the change in structural estimation error with large and refined domains of uncertainty.

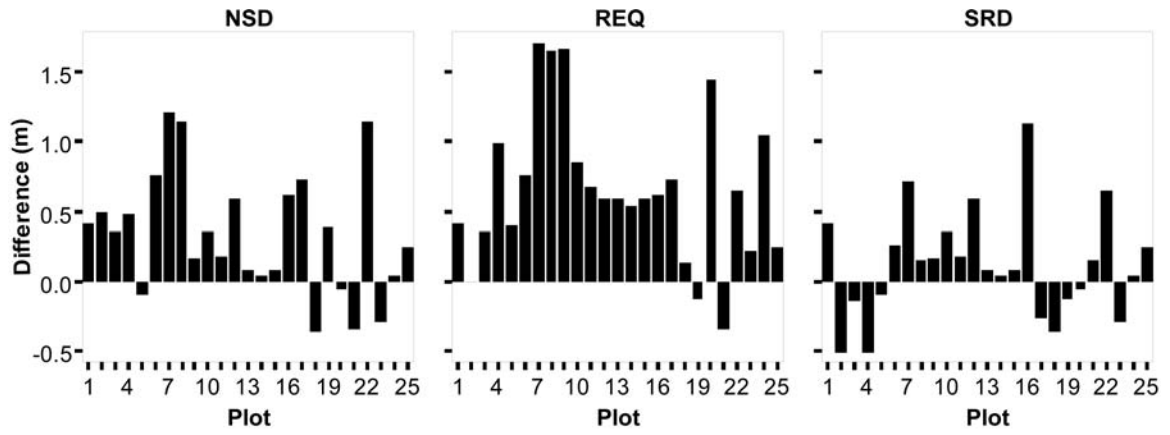

Figure 5. Difference between predicted and measured horizontal crown radius for 25 plots for nearest spectral distance (NSD), reflectance equality (REQ), and spectral range domain (SRD). Results based on lowest overall absolute RMSE.

solutions, and any error domain size is reasonable, then the inversion method has been successful. A statistical summary of the distribution of potential solutions using central tendency functions may not capture the best (or "true") matching value with respect to the field validation. Accordingly, the actual quality of result available using MFM may be higher than central tendency based results reported here. The use of central tendency also makes assumptions about the nature of the distribution of potential solutions and the location of the measured value within. Depending on model sensitivity, it is also possible that returns within a spectrally equidistant domain will not be normally distributed and may render central tendency measures less effective. Accordingly, the distribution of potential solutions was examined to determine if the actual field-measured value could be found within the solution set. The level of uncertainty, as it was related to the extents of the distribution of solutions, was also examined through these distributions. A sample of eight randomly selected validation plots, including those with high and low error, were examined using a two-band spectral domain case.

With the exception of vertical crown radius in field plot 4, all measured values were found near or within the distribution of potential solutions (Figures 7 and 8). These results also demonstrated that there was a difference in some plots (e.g., plots 4, 7, 16, and 22) between measured values and those reported when the distribution was summarized using central tendency for reporting purposes. These plots corresponded to those with higher error levels (Figures 5 and 6). This error was reported despite the fact that the actual measured value was still found in the distribution. While strictly reporting the central tendency measures is not incorrect per se, these results suggested that distributions of solutions may yield additional information regarding the range of values the estimate may potentially occupy.

Producing these distributions also demonstrated the differences in solution sets with regard to change in spectral domain size. For example, when the relative RMSE was set to 0.4, a wide distribution of potential solutions was displayed since a considerable amount of the LUT was selected as a match (Figure 9). As the spectral distance was decreased,

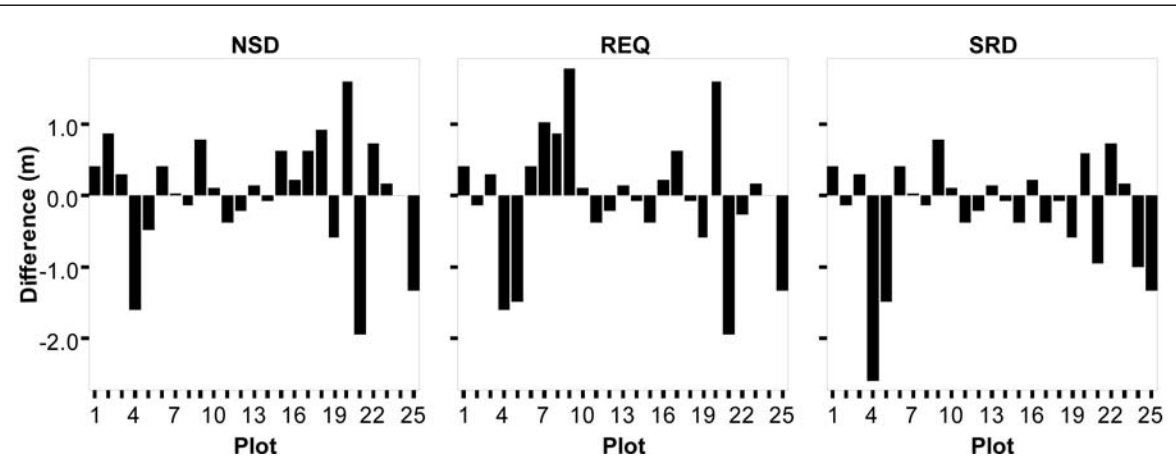

Figure 6. Difference between predicted and measured vertical crown radius for 25 plots for nearest spectral distance (NSD), reflectance equality (REQ), and spectral range domain (SRD). Results based on lowest overall absolute RMSE.

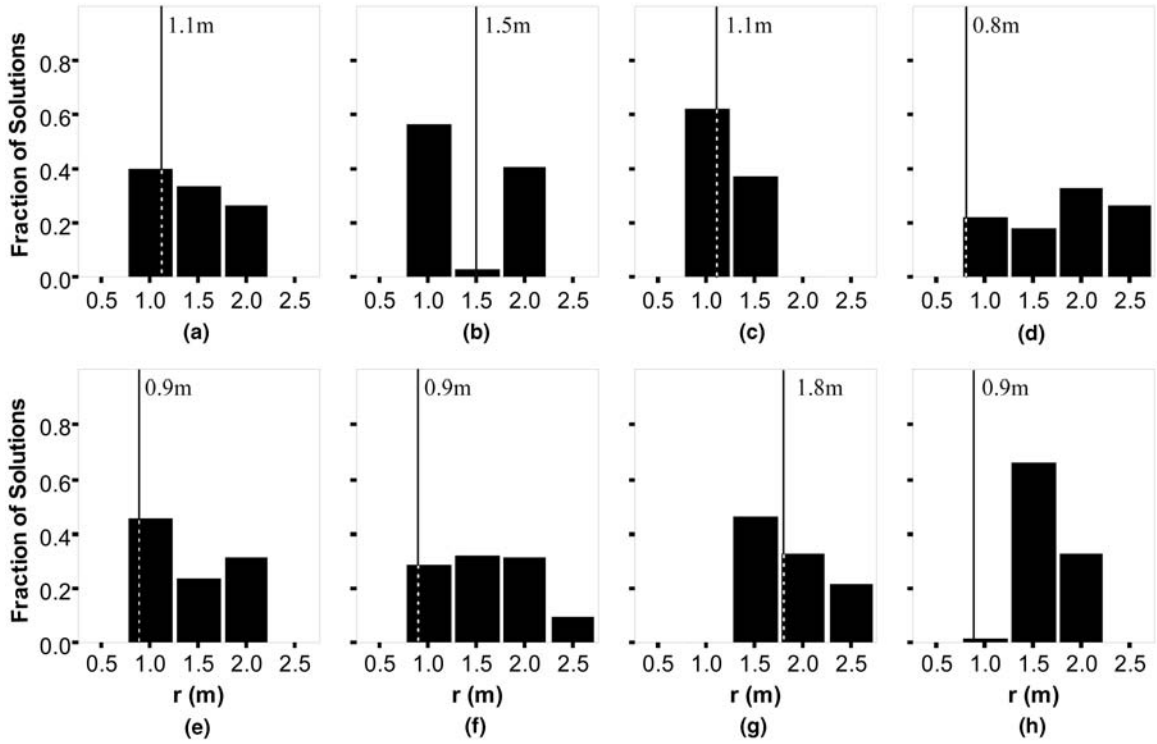

Figure 7. Distribution of potential solutions for horizontal crown radius using a 0.05 relative RMSE spectral domain: (a) Plot 1, (b) Plot 4, (c) Plot 5, (d) Plot 7, (e) Plot 8, (f) Plot 16, (g) Plot 17, and (h) Plot 22. Vertical line with label indicates field measured structural value.

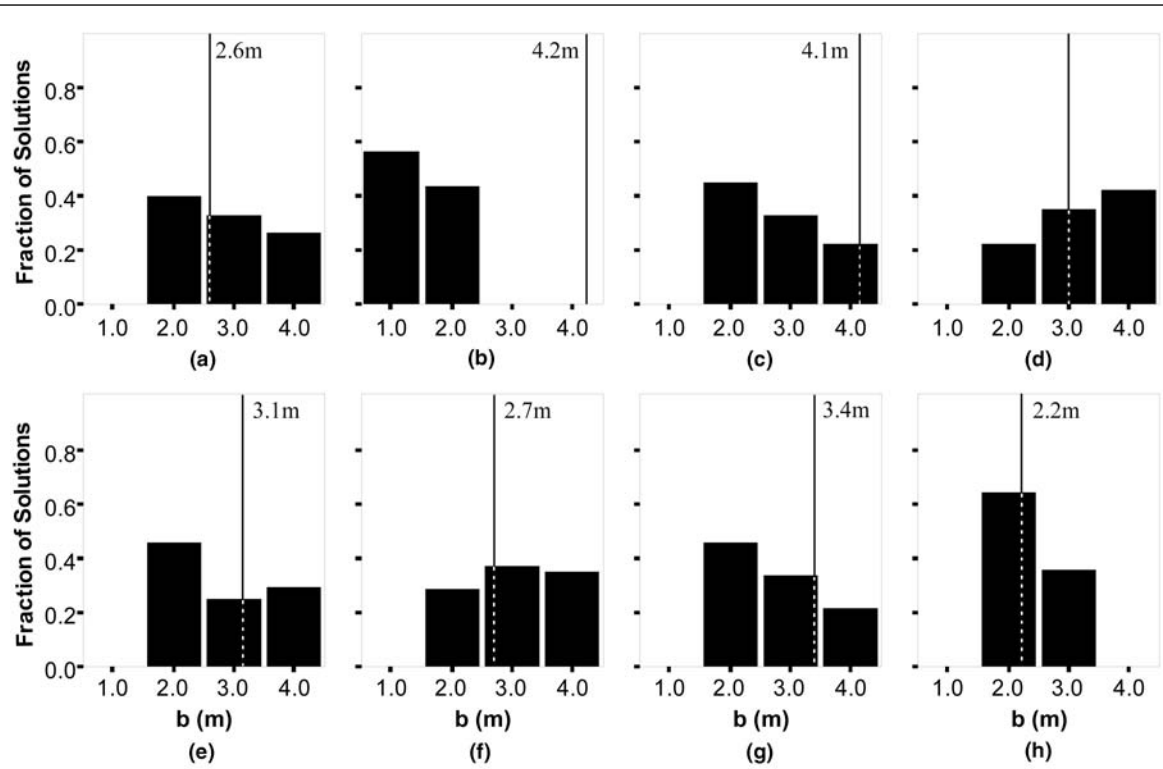

Figure 8. Distribution of potential solutions for vertical crown radius using a 0.05 relative RMSE spectral domain: (a) Plot 1, (b) Plot 4, (c) Plot 5, (d) Plot 7, (e) Plot 8, (f) Plot 16, (g) Plot 17, and (h) Plot 22. Vertical line with label indicates field measured structural value.

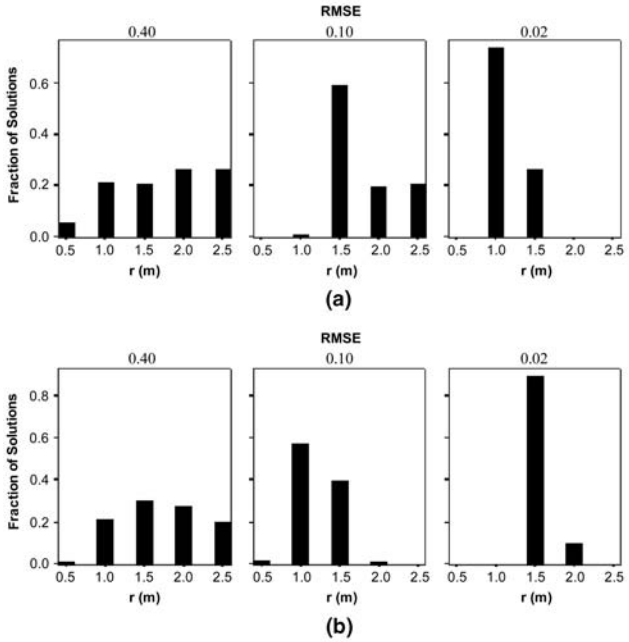

Figure 9. Distribution of potential solutions of horizontal crown radius from MFM run 4 LUTs for two conifer plots using two spectral input channels with varying spectral distance ranges (relative RMSE 0.4, 0.1, 0.02). Average field measured values of horizontal crown radius: (a) 1.2 m (min: 0.6, max 2.0), and (b) 1.3 (min: 0.9, max: 2.3).

the distribution converged towards the correct value. This continues until an error threshold is reached. If the spectral distance is within the error threshold, the "correct value" still falls within the distribution of values. In this form of assessment, the correspondence between solution distributions at lower relative RMSE ranges and the minimum and maximum field measured values should be noted.

Conclusions

Three variations of an indirect inversion method for a geometric optical canopy reflectance model were tested and evaluated based on ability to estimate horizontal and vertical crown structural dimensions in a mountain coniferous forest. Conceptually, the approaches developed here provide flexibility and power within a canopy reflectance model inversion context for extracting detailed biophysical structural information. These approaches were shown to provide improved quality and diversity of forest information for an area of complex mountainous terrain. The ability to estimate these parameters was a function of the information content of the LUT sets used in the indirect inversion procedure. The mean estimate error for the field plots showed dependency with the MFM input increment size, with error decreasing with smaller increment sizes. Estimates taken from LUTs generated using *in situ* knowledge were also slightly more accurate than those from LUTs using unrefined ranges. When coarser increments and ranges were used, the content was less focused within the image domain where there was a high density of *d*.

Use of additional spectral information bands improved estimates when the NSD retrieval method was used. When additional information bands were used in the REQ method there was an increase in "no match" cases (i.e., where there was no matching reflectance between modeled and image data). For the SRD method, using additional spectral inputs and terrain data to constrain potential matches did not consistently improve estimates. This was likely due to the generalized input structure created by compromising LUT detail for computational efficiency. However, it should be noted that the use of DEM input did not significantly increase the level of error found in the estimates. Increases in error were typically less than 30 cm.

The results also suggested that a spectral distance function approach to indirect inversion is preferable to a strict REQ approach. This was because the estimates maintained a similar or improved level of accuracy when comparing the spectral distance method in situations where a full set of estimates was returned within the reflectance equality method. The spectral distance function has two primary advantages: (a) the ability to indirectly account for domains of uncertainty, and (b) the ability to provide potential solution information focused within a user defined spectral range. With the spectral distance function, it was also possible to explore distributions of potential solutions which yield more information regarding surface conditions compared to summaries of the solution sets achieved through indirect inversion.

This study shows the potential to extract specific, accurate structural information. While it has become common practice to summarize distributions such as solution sets using measures of central tendency, and to then use those summary statistics in validations against field data, we have shown here that this often results in overestimations in reported error (i.e., in reality, the MFM model error is less than that reported based on central tendency distribution generalizations). Modeled output contains the exact match, or closer matches, than those indicated by simple summary statistics. In addition, the method presented here is not model specific and therefore may be applied to canopy reflectance models that provide a more detailed description of the radiative transfer process. Future work will focus on additional applications and refinements to the MFM algorithm, including the use of more advanced statistical methods to describe and summarize the distribution of potential solutions.

Acknowledgments

This research was supported in part by grants to Dr. Peddle and collaboration from the Natural Sciences and Engineering Research Council of Canada (NSERC), Alberta Ingenuity Centre for Water Research (AICWR), Prairie Adaptation Research Collaborative (PARC), Water Institute for Semiarid Ecosystems (WISE), Natural Resources Canada, NASA Goddard Space Flight Centre/University of Maryland, Alberta Research Excellence Program, Miistakis Institute of the Rockies (DEM), Center for Remote Sensing, Boston University (GOMS model), and the University of Lethbridge. Computing resources were provided through the Western Canada Research Grid (WestGrid NETERA c3.ca). SPOT imagery was acquired from Iunctus Geomatics Corporation and the Alberta Terrestrial Imaging Centre (ATIC), both of Lethbridge Alberta. We are grateful to Sam Lieff, Adam Minke, and Kristin Yaehne for field assistance and the staff at the Kananaskis Field Stations for logistical support in the field.

References

Abuelgasim, A.A., and A.H. Strahler, 1994. Modeling bidirectional radiance measurements collected by the advanced solid-state

array spectroradiometer (ASAS) over Oregon transect conifer forests, *Remote Sensing of Environment*, 47:261–275.

Archibald, J.H., G.D. Klappstein, and I.G.W. Corns, 1996. *Field Guide to Ecosites of Southwestern Alberta*, UBC Press, Vancouver, British Columbia, 523 p.

Bannari, A., D. Morin, F. Bonn, and A.R. Huete, 1995. A review of vegetation indices, *Remote Sensing Reviews*, 13:95–120.

Brown, S., 2002. Measuring carbon in forests: Current status and future challenges, *Environmental Pollution*, 116:363–372.

Chen, J.M., X. Li, T. Nilson, and A. Strahler, 2000. Recent advances in geometrical optical modelling and its applications, *Remote Sensing Reviews*, 18:227–262.

Combal, B., F. Baret, M. Weiss, A. Tubuil, D. Mace, A. Pragnere, R. Myeni, Y. Knyazikhin, and L. Wang, 2002. Retrieval of canopy biophysical variables from bidirectional reflectance using prior information to solve the ill-posed inverse problem, *Remote Sensing of Environment*, 84:1–15.

Curran, P.J., and H.D. Williamson, 1987. GLAI estimation using measurements of red, near infrared, and middle infrared radiance, *Photogrammetric Engineering & Remote Sensing*, 53(1):181–186.

Fournier, R.A., J.E. Luther, L. Guindon, M.-C. Lambert, D. Piercey, R.J. Hall, and M.A. Wulder, 2003. Mapping above ground tree biomass at the stand level from inventory information: Test cases in Newfoundland and Quebec, *Canadian Journal of Forest Research*, 33:1846–1863.

Franklin, S.E., 2001. *Remote Sensing for Sustainable Forest Management*, Lewis Publishers, Boca Raton, Florida, 406 p.

Gastellu-Etchegorry, J.P., F. Gascon, and P. Esteve, 2003. An interpolation procedure for generalizing a look-up table inversion method, *Remote Sensing of Environment*, 87:55–71.

Gemmell, F., 1998. An investigation of terrain effects on the inversion of a forest reflectance model, *Remote Sensing of Environment*, 65:155–169.

Gong, P., and B.Xu, 2003. Remote sensing of forests over time: Change types, methods, and opportunities, Chapter 11, *Remote Sensing of Forest Environments: Concepts and Case Studies* (M.A. Wulder and S.E. Franklin, editors) Kluwer Academic Press, Norwell, Massachusetts, pp.301–334.

Guyot, G.D., D. Guyon and D.G. Riom, 1989. Factors affecting the spectral response of forest canopies: A review, *Geocarto International*, 3:3–18.

Hall, F.G., Y.E. Shimabukuro, and K.F. Huemmrich, 1995. Remote sensing of forest biophysical structure in boreal stands of picea mariana using mixture decomposition and geometric reflectance models, *Ecological Applications*, 5:993–1013.

Hall, F.G., D.R. Peddle, and E.F. LeDrew, 1996. Remote sensing of biophysical variables in boreal forest stands of *Picea mariana, International Journal of Remote Sensing: Letters*, 17:3077–3081.

Hall, F.G., 1999. BOREAS in 1999: Experiment and science overview, *Journal of Geophysical Research*, 104(D22):27627–27639.

Kimes, D.S., Y. Knyazikhin, J. Privette, A. Abuelgasim, and F. Gao, 2000. Inversion methods for physically based models, *Remote Sensing Reviews*, 18:381–440.

Knyazikhin, Y., J.V. Martonchik, D.J. Diner, R.B. Myeni, M. Verstraete, B. Pinty, and N. Gobron, 1998. Estimation of vegetation canopy leaf area index and fraction of absorbed photosynthetically active radiation from atmosphere-corrected MISR data, *Journal of Geophysical Research*, 103(D24):32239–32256.

Lathrop, R.G., and L.L. Pierce, 1991. Ground-based canopy transmittance and satellite remotely sensed measurements for estimation of coniferous forest canopy structure, *Remote Sensing of Environment*, 36:179–188.

Li, X., and A.H. Strahler, 1992. Geometric-optical bidirectional reflectance modeling of the discrete crown vegetation canopy: effect of crown shape and mutual shadowing, *IEEE Transactions on Geoscience and Remote Sensing*, 30:276–292.

McDonald, A.J., F.M. Gemmell, and P.E. Lewis, 1998. Investigation of the utility of spectral vegetation indices for determining information on coniferous forests, *Remote Sensing of Environment*, 66:250–272.

Milton, E.J., K. Lawless, A. Roberts, and S.E. Franklin, 1997, The effect of unresolved scene elements on the spectral response of calibration targets: An example, *Canadian Journal of Remote Sensing*, 23(3):126–130.

Patenaude, G., R. Milne, and T. Dawson, 2005. Synthesis of remote sensing approaches for forest carbon estimation: Reporting to the Kyoto Protocol, *Environmental Science and Policy*, 8:161–178.

Peddle, D.R., F.G. Hall, and E.F. LeDrew, 1999. Spectral mixture analysis and geometric-optical reflectance modeling of boreal forest biophysical structure, *Remote Sensing of Environment*, 67:288–297.

Peddle, D.R., S.P. Brunke and F.G. Hall, 2001a. A comparison of spectral mixture analysis and ten vegetation indices for estimating boreal forest biophysical information from airborne data, *Canadian Journal of Remote Sensing*, 27:627–635.

Peddle, D.R., H.P. White, R.J. Soffer, J.R. Miller, and E.F. LeDrew, 2001b. Reflectance processing of remote sensing spectroradiometer data, *Computers and Geosciences*, 27:203–213.

Peddle, D.R., S.E. Franklin, R.L. Johnson, M.A. Lavigne, and M.A. Wulder, 2003a. Structural change detection in a disturbed conifer forest using a geometric optical reflectance model in multiple forward mode, *IEEE Transactions in Geoscience and Remote Sensing*, 41:163–166.

Peddle, D.R., P.M. Teillet, and M.A. Wulder, 2003b. Radiometric image processing, Chapter 7, i *Remote Sensing of Forest Environments: Concepts and Case Studies* (M.A. Wulder and S.E. Franklin, editors) Kluwer Academic Press, Norwell, Massachusetts, pp.181–208.

Peddle, D.R., J.E. Luther, N. Pilger, and D. Piercey, 2003c. Forest biomass estimation using a physically-based 3D-structural modeling approach for Landsat TM cluster labeling, *Proceedings of the 25th Canadian Symposium on Remote Sensing*, 14–17 October, Montreal, Quebec, Canadian Aeronautics and Space Institute, Ottawa, unpaginated CD-ROM.

Peddle, D.R., R.L. Johnson, J. Cihlar, and R. Latifovic, 2004. Large area forest classification and biophysical parameter estimation using the 5-scale canopy reflectance model in multiple-forward-mode, *Remote Sensing of Environment*, 89:252–263.

Peddle, D.R., R.L. Johnson, J. Cihlar, S.G. Leblanc, J.M. Chen, and F.G. Hall, 2007. Physically-based inversion modeling for unsupervised cluster labeling, independent forest classification and LAI estimation using MFM-5-Scale, *Canadian Journal of Remote Sensing*, 33(3):214–225.

Pilger, N., D.R. Peddle and R.J. Hall, 2003. Forest volume estimation using a canopy reflectance model in multiple-forward-mode, *Proceedings of the 25th Canadian Symposium on Remote Sensing*, 14–17 October, Montreal, Quebec, Canadian Aeronautics and Space Institute, Ottawa, unpaginated CD-ROM.

Riano, D., E. Chuvieco, S. Condes, J. Gonzalez-Matesanz, and S. Ustin, 2004. Generation of crown bulk density for *Pinus sylvestris* L. from lidar, *Remote Sensing of Environment*, 92:345–352.

Rosenqvist, A., A. Milne, R. Lucas, M. Imhoff, and C. Dobson, 2003. A review of remote sensing technology in support of the Kyoto Protocol, *Environmental Science & Policy*, 6:441–455.

Schaff, C.B., X. Li, A.H. Strahler, 1994. Topographic effects on bidirectional and hemispherical reflectances calculated with a geometric-optical canopy model, *IEEE Transactions on Geoscience and Remote Sensing*, 32:1186–1193.

Schaff, C.B., and A.H. Strahler, 1994. Validation of bidirectional and hemispherical reflectances from a geometric-optical model using ASAS imagery and pyranometer measurements of a spruce forest, *Remote Sensing of Environment*, 49:138–144.

Smith, G.M., and .E.J. Milton, 1999. The use of the empirical line method to calibrate remotely sensed data to reflectance, *International Journal of Remote Sensing*, 20:2653–2662.

Sellers, P.J., 1985. Canopy reflectance, photosynthesis, and transpiration, *International Journal of Remote Sensing*, 6:1335–1372.

Soenen, S.A., D.R. Peddle, and C.A. Coburn, 2005. SCS + C: A modified sun-canopy-sensor topographic correction in forested terrain, *IEEE Transactions on Geoscience and Remote Sensing*, 43:2148–2159.

Soenen, S.A., D.R. Peddle, C.A. Coburn, R.J. Hall, and F.G. Hall, 2008. Improved topographic correction of forest image data using a 3-D canopy reflectance model in multiple forward mode, *International Journal of Remote Sensing*, 29(4) 1007–1027.

Spanner, M.A., L.L. Pierce, D.L. Peterson, and S.W. Running, 1990. Remote sensing of temperate coniferous forest leaf area index: The influence of canopy closure, understory vegetation and background reflectance, *International Journal of Remote Sensing*, 11:95–111.

Strahler, A.H., 1997. Vegetation canopy reflectance modeling – Recent developments and remote sensing perspectives, *Remote Sensing Reviews*, 15:179–194.

UNFCCC, 1998. Kyoto Protocol to the United Nations Framework Convention on Climate Change, URL: *http://unfccc.int/resource/docs/convkp/kpeng.pdf*, United Nations (last date accessed: 26 September 2008).

UNFCCC, 2004. Implementation plan for the Global Observing System for Climate in support of the UNFCCC, *Final Report, United Nations Framework Convention on Climate Change*, 06–17 December, Buenos Aires, UNFCCC, WMO/TD No. 1219, United Nations, New York, pp. 1–143.

Weiss, M., F. Baret, R.B. Myneni, A. Pragnere, and Y. Knyazikhin, 2000. Investigation of a model inversion technique to estimate canopy biophysical variables from spectral and directional reflectance data, *Agronomie*, 20:3–22.

(Received 23 February 2007; accepted 14 May 2007; revised 23 October 2007)